Anchoring 2D Metal-Organic Frameworks (MOFs) for Electrochemical Energy Storage: Recent Advances, Challenges and Key Applications

Rahul Mitra [1, 3, #], Swagatika Mohanty [2, 3, #], Unnikrishnan Manju [1, 3, *]

[1] Materials Chemistry Department, CSIR-Institute of Minerals and Materials Technology, Bhubaneswar - 751 013, India

[2] Central Characterization Department, CSIR-Institute of Minerals and Materials Technology, Bhubaneswar - 751 013, India

[3] Academy of Scientific and Innovative Research (AcSIR), Ghaziabad - 201 002, India

**Corresponding author: manju@immt.res.in, orcid.org/0000-0001-9842-6648*

Abstract

Two-dimensional (2D) materials have received a lot of interest in recent years due to their distinctive properties and staggering potential in energy storage systems. Due to its propensity to support electrochemically active sites that increase the capacity for charge storage, 2D metal-organic frameworks (MOFs) have risen in prominence. It alludes to a novel family of 2D materials that can provide distinct open channels and regular active sites. However, a limited number of articles have revealed how 2D MOFs offer attributes that can improve the functionality of energy storage devices. In this study, we have outlined the structure and state-of-the-art synthesis strategies of 2D MOFs and their use as energy storage devices in supercapacitors and batteries. Finally, key challenges and limitations are addressed while the future view offers a comprehensive idea and a fresh perspective for potential future research possibilities to use this family of materials in energy storage applications. These 2D-MOFs are excellent for energy applications owing to their exceptional qualities, including swift charge and discharge, phenomenal power density, and longer life cycles.

Keywords: *2D materials, Metal-organic frameworks, Batteries, Supercapacitors, Electrochemical Storage*

1. Introduction

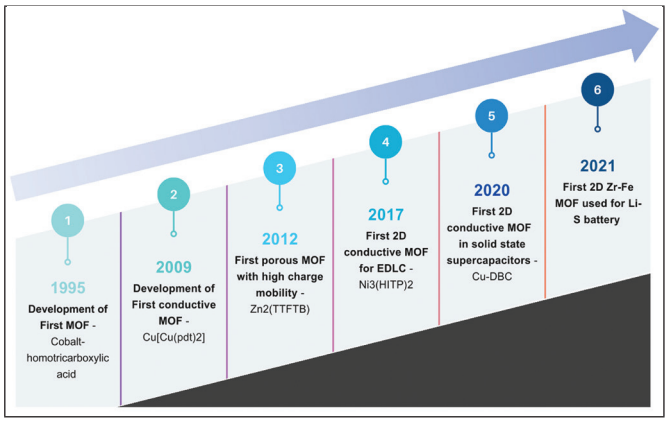


Fig. 1 Schematic representation of major milestones in the development of MOFs. [1–10]

Metal-organic frameworks (MOFs) have attracted increasing attention due to their porous structure, thermal stability, adaptable surface chemistry, robust configuration, and high surface area [11–13]. These materials are formed by the interconnection of metal ions and organic ligands through coordination bonds. The flexible nature of MOF structures allows for regulation by modifying the type of metal cation and organic linkers. The synthesis process also plays a crucial role in determining the morphology and structure of MOFs [14]. Since the synthesis of the first metal-organic framework material, layered cobalt-homophonic acid, in 1995, more than 20,000 MOFs have been reported as of 2022, with the major

milestones depicted in Fig. 1 [1–10]. These materials have found widespread applications in catalysis, sensing, separation, and energy storage systems, that have led to numerous contributions in the scientific fields in terms of publications from across the world and its year-on-year growth, as compiled from Web of Science in Figs. 2(a-c) [2,15,16]. However, traditional 3D MOFs synthesized in the past have inherent limitations that hinder their extensive use in electrochemical energy storage. These drawbacks include sensitivity to moisture, reduced capacity in humid conditions, poor electrical conductivity leading to subpar rate performance, and narrow micropores that limit rapid ion diffusion, affecting their ion storage capabilities [17,18]. Moreover, the incomplete exposure of active sites in the common 3D MOF morphologies, characterized by a 3D frame, restricts contact with diffusing ions, thereby impairing electrochemical performance.

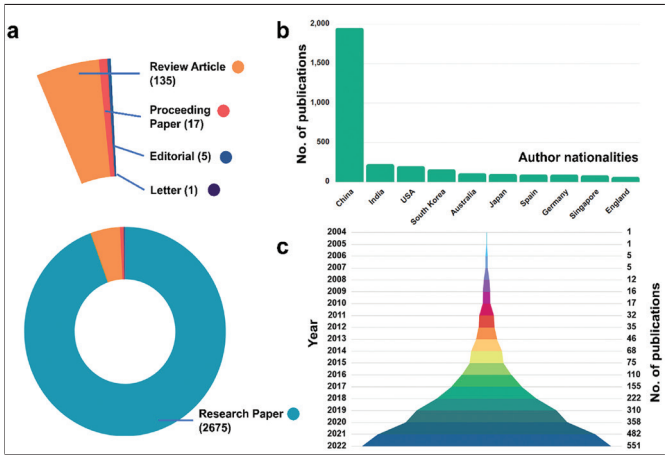


Fig. 2 (a) Pie chart showing the distribution of research article types in the field of 2D MOFs. (b) Number of publications vs Associated author nationalities and (c) Year-wise distribution of publications in the field showing an ever-increasing trend in the last 20 years.

Due to these shortcomings, 3D MOFs have seldom been directly employed as energy storage materials. Fortunately, the porous skeleton structure and pore size of MOFs are adjustable, offering opportunities to enhance their electrochemical performance as electrode materials for energy storage devices. This can be achieved by improving MOF conductivity and optimizing their structural characteristics.

In the current landscape of energy storage technologies, both supercapacitors and batteries play pivotal roles, each with distinct advantages and challenges. Supercapacitors excel in high-power applications due to their rapid charge and discharge rates but face limitations in energy density [19–21]. On the other hand, batteries provide higher energy density but often have slower kinetics and may suffer from issues related to cycle life and safety [22–26]. Achieving optimal properties such as high specific capacitance, extended cycle life, and enhanced energy density remains a central focus for both supercapacitors and batteries. In this context, MOFs exceedingly emerge as a compelling avenue for investigation. MOFs exhibit unique structural features, including high surface area, tunable porosities, and versatile chemical compositions, making them promising candidates for addressing the challenges in both supercapacitors and batteries. The tunable nature of MOFs allows for the design of materials with tailored redox potentials, facilitating improved energy storage capabilities in supercapacitors. Additionally, the porous nature of MOFs provides opportunities for efficient ion transport and storage, enhancing the performance of batteries. The integration of MOFs into these energy storage devices holds potential for advancing the efficiency and sustainability of emerging technologies, offering a bridge between the traditionally separate domains of supercapacitors and batteries. The investigation of MOFs in this context is driven by the prospect of harnessing their unique properties to overcome existing limitations, ultimately contributing to the development of next-generation energy storage systems that balance power and energy density while promoting sustainability in the face of increasing global energy demands.

In this review, we have extensively summarized a range of preparation techniques for two-dimensional metal-organic frameworks (2D MOFs). These methods encompass both top-down approaches and bottom-up strategies, providing a foundational understanding for the precise fabrication of 2D MOFs within advanced energy storage systems.

Furthermore, we have conducted a systematic analysis of the recent research progress concerning the utilization of 2D MOFs in energy storage applications, with a particular focus on their roles in supercapacitors and various battery configurations. Finally, we have highlighted the current limitations in existing research efforts and proposed future directions for the development of 2D MOFs in the field of energy storage, with the aim of advancing energy storage systems to their full potential. The complete overview is represented as a bubble chart in Fig. 3.

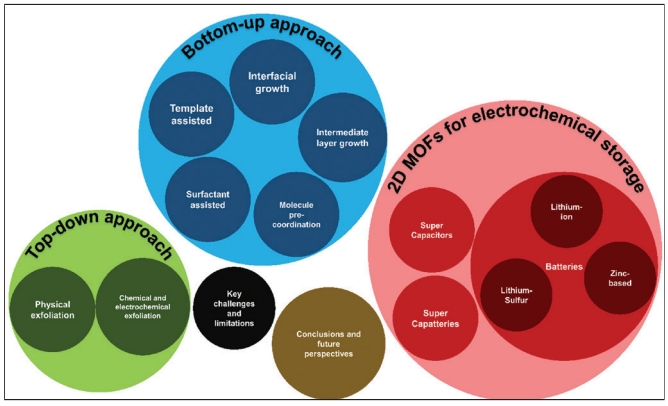


Fig. 3 Bubble chart illustrating the sections and classifications in the review.

2. Synthesis strategies of 2D MOFs

2.1 Top-down approach

2.1.1 Physical exfoliation method

The exfoliation of 2D MOF nanosheets from their layered bulk MOF into single- or few-layers is crucial for realizing the full potential of these MOF nanosheets since structural degradation and morphological damage have made it difficult to produce high-quality MOF nanosheets during exfoliation [27–29]. Soft-physical exfoliation is one of the most often utilized synthetic techniques for obtaining ultrathin nanosheets due to its ease of usage and amiable circumstances. In neutral layered MOFs, the weak connections between layers can then be selectively torn apart by ultrasonic vibration to accomplish exfoliation.

Han et al. synthesized a novel layered bulk 2D MOF ZSB-1 ($Zn_2(SBA)_2(BPTP)$, SBA = 4,4′-sulfonylbibenzoic acid, BPTP = 3,5-bis(5-(pyridin-4-yl) thiophen-2-yl)pyridine) using the top-down physical exfoliation strategy [30]. Using a top-down liquid ultrasonication exfoliation technique, ZSB-1 nanosheets were prepared, where wet powder of ZSB-1 (10 mg, ground for 1 hour in n-hexyl alcohol) was ultrasonically processed in n-hexyl alcohol (80 mL) for 36 hours at room temperature. The upper-layer colloidal suspension was obtained by centrifuging the milky colloidal suspension at 4000 rpm for 10 minutes, and the ZSB-1 nanosheet materials were obtained by centrifuging at 14000 rpm for 5 minutes. The schematic representation of the physical exfoliation method using solvothermal synthesis is depicted in Fig. 4(a).

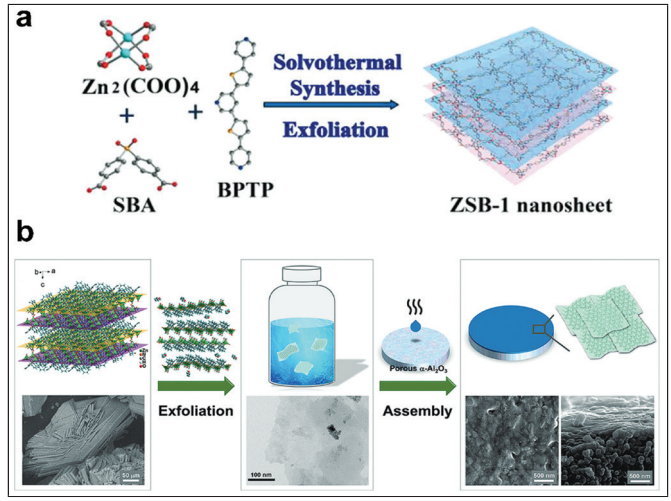


Fig. 4 (a) Schematic illustration of the synthesis process of ZSB-1 nanosheets employing top-down physical exfoliation. [30] (b) Precursor exfoliation and nanosheet assembly processes of $Zn_2(Bim)_3$ nanosheets. [31]

For the first time, $[Zn_2(benzimidazole)_3(OH)(H_2O)]_n$ nanosheets ($Zn_2(Bim)_3$) were prepared by Peng et al. using a modified top-down technique from layered $Zn_2(Bim)_3$ precursors [31]. Each Zn ion acts as a metallic node in the layered structure, coupled by three benzimidazole ligands, and each benzimidazole connects two Zn ions by a bis-monodendate connection, generating a structure resembling a six-membered ring pore opening. Each Zn ion's remaining dangling bond is filled with H_2O molecules, which primarily come from zinc nitrate hexahydrate. In the interlayer gap of bulk precursors, free water molecules and N,N-

dimethylformamide (DMF) are present. All the benzimidazole ligands are placed on one side of a single-layered nanosheet, and the coordinated water is arranged on the opposite side. They attempted to build these nanosheets on asymmetric α-Al_2O_3 porous substrates using a simple hot-drop coating approach at various coating temperatures after successfully disintegrating $Zn_2(Bim)_3$ precursors into nanosheets. For a better comprehension of the exfoliation and nanosheet building processes, a flowchart is provided in Fig. 4(b).

2.1.2 Chemical and electrochemical exfoliation methods

Current research efforts in MOF exfoliation have mainly concentrated on isolating 2D frameworks held together by interlayer van der Waals forces or hydrogen bonding in bulk crystals [14,32–35]. However, the lack of precise control over the mechanical or solvent-driven exfoliation process, which relies on weakening interlayer interactions in MOF crystals, often results in the production of 2D nanosheets with varying thicknesses and low yields. To address this issue, there is a growing need for a more dependable exfoliation approach that leverages controlled chemical reactions to modulate interlayer interactions. One efficient method for producing ultrathin 2D inorganic nanosheets involves the exfoliation of layered inorganic solids that have been pre-intercalated through chemical means [36,37].

Specifically, Ding et al. presented a novel method for the high-yield production of 2D MOF nanosheets from intercalated MOF crystals via chemical exfoliation [38]. They added a chemically labile dipyridyl ligand, 4,4′-dipyridyl disulfide (DPDS), to the layered MOF crystals to create new intercalated MOFs in order to create chemically sensitive MOFs. MOFs may be readily exfoliated into ultrathin 1 nm nanosheets in high yield (~57%) because the interlayer contacts between expanding 2D layers are decreased following scissoring of DPDS by chemically reducing the disulfide bond using trimethylphosphine (TMP). They also showed that the nanosheets as made had extremely high singlet oxygen ($^1O_2$) production efficiency for heterogeneous photocatalysis.

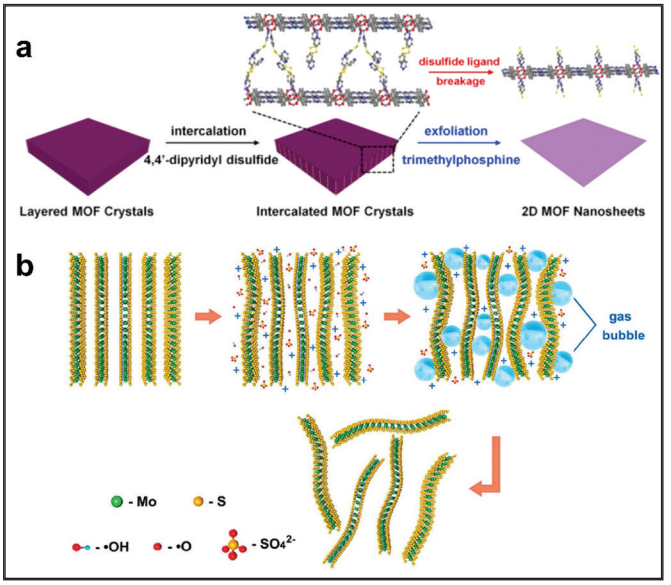


Fig. 5 (a) Standard method designed to create 2D MOF nanosheets by chemical exfoliation and intercalation approach. [38] (b) Mechanism of electrochemical exfoliation of MoS_2 flakes using Na_2SO_4 solution. [39]

Fig. 5(b) explains the electrochemical exfoliation process of MoS_2 crystals using electrochemical exfoliation approach, adopted by Liu et al [39]. First, the oxidation of water results in OH and O radicals gathered around the MoS_2 crystal when a positive bias is applied to the working electrode. The van der Waals contacts between the MoS_2 layers are weakened as a result of the OH and O radicals and/or SO_4^{2-} anions inserting themselves between the layers. Second, the release of O_2 and/or SO_2 from the oxidation of the radicals and/or anions results in a significant expansion of the MoS_2 interlayers. Finally, the exploding gas separates the MoS_2 flakes from the MoS_2 crystal, which are subsequently suspended in the solution. The generalized electrochemical exfoliation approach can, therefore, be extended for the top-down synthesis of 2D MOFs as well.

2.2 Bottom-up approach

2.2.1 Template-assisted methods

The bottom-up template-assisted method offers precise control over the structure and properties of MOFs, making it a valuable tool in materials science and chemistry. By selecting the appropriate template and building blocks, researchers can tailor

the MOF to meet specific application requirements. This method allows for the creation of MOFs with well-defined pore sizes, surface areas, and chemical functionalities, enhancing their performance in various industrial and scientific applications. The creation of an N,O-doped mesoporous carbon nanosheet using a template-assisted technique for morphology assembly from a solvent dispersible hydroxyquinoline-Zn combination was initially described by Wei et al. A self-assembled $Mg(OH)_2$ with a sheet-like shape was used as the template, and 5,7-dibromo-8-hydroxyquinoline-Zn was created and used as the precursor. The hydroxyquinoline-Zn combination serves as both a carbon supply and a sacrificial template in the design, employing the ZnO nanoparticles produced during carbonization as a model for the development of mesoporosity, the schematic for which is depicted in Fig. 6(a).

H_2pyip has a carboxylate O atom and a pyridine N atom, which results in a variety of coordination modes and strong coordination abilities with regard to metal ions, making it an effective ligand for creating MOFs with intriguing structures and potential features. When $MnCl_{24}H_2O$ and 4,4′-bipyridyl were used as a template by Liu et al., $[Mn_3(pyip)_2(HCOO)_2(H_2O)_2]_n$ was produced at 120 °C [40]. Using $Co(NO_3)_2.6H_2O$ and cyanoacetic acid as a template, $\{[Co(pyip)(H_2O)].H_2O\}_n$ was produced at 130 °C. No crystals or precipitates formed during the reactions when the templating agent was not present. This observation suggests that the role of the templating agents in the development of these MOFs was significant.

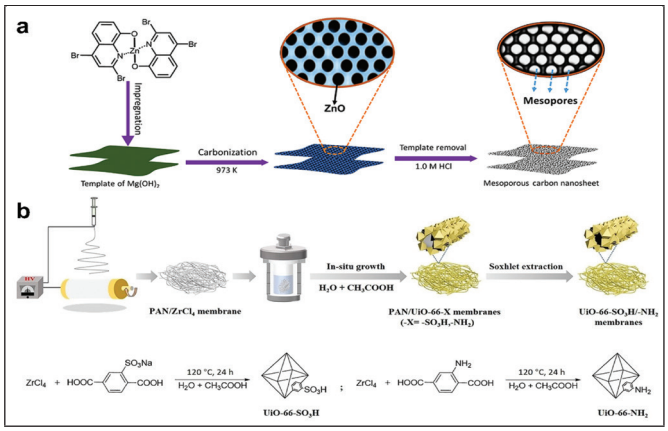


Fig. 6 (a) Schematic of hydroxyquinoline-Zn combination used to create mesoporous carbon nanosheets. [40] (b) The technique to construct the self-standing UiO-66-SO_3H and UiO-66-NH_2 membranes, as well as the procedure for making the matching MOFs. [41]

Fig. 6(b) depicts the process used to create individual porous membranes with base-functionalized MOF (UiO-66-NH_2) and acid-functionalized MOF (UiO-66-SO_3H) structures, as investigated by Du et al [41]. First, by electrospinning a combined solution of $ZrCl_4$ and PAN in DMF, a fiber membrane made of polyacrylonitrile (PAN) and $ZrCl_4$ was created. The non-woven membrane was created by the random deposition of fibers with an average diameter of 500 nm and a thickness of ~80 μm. Then, using the in-situ growth approach, MOF (UiO-66-SO_3H and UiO-66-NH_2) were formed on PAN membrane using either the 2-aminobenzenedicarboxylic acid (BDC-NH_2) or 2-sulfobenzenedicarboxylic acid monosodium salt (BDC-SO_3Na) and an acetic acid catalyst in the water. The membranes effectively accelerated the two phases of a cascade one-pot reaction, namely the reaction of the active methylene molecules malononitrile and ethyl cyanoacetate with benzaldehyde and the deacetylation of benzaldehyde dimethyl acetal to benzaldehyde. The end product might have a high overall yield. As catalysts for the reaction of benzaldehyde with active methylene compounds possessing high p*K*a, such as diethyl malonate, MOF membranes containing -NH_2 base groups are only often used [42,43].

2.2.2 Interfacial or Intermediate layer growth methods

In this method, 2D MOFs are synthesized by carefully controlling the growth of MOF layers at the interface of two immiscible phases. This technique allows for precise control over the formation of 2D MOF nanosheets with tailored properties. Like in other MOF synthesis methods, the first step involves selecting suitable metal ions (or metal clusters) and organic ligands (or linkers) that will constitute the 2D MOF [44,45]. These components are chosen based on the desired MOF structure and properties. The key feature is the use of two immiscible phases, typically a liquid-liquid or liquid-solid interface.

One phase contains the metal ions or clusters, while the other phase contains the organic ligands or linkers. A precursor solution is prepared by dissolving the metal ions or clusters in one phase and the organic ligands in the other phase [46,47]. These solutions are designed to react and form the MOF at the interface. The two immiscible phases are brought into contact at the interface, typically in a controlled manner.

Notably, Cu-MOF nanosheets were produced by sonication exfoliation of Cu-MOF membranes after first being created by interfacial growth, which layers the organic phase on the aqueous phase by Wu et al [48]. Four $Cu_2(COO)_4$ paddlewheel metal nodes connected crystals of Cu-MOF nanosheets bearing tetrakis(4-carboxyphenyl)porphyrin (TCPP) ligands to create a layered, checkerboard-like structure, as observed in Fig. 7(a). As anticipated, after 3 days, discolouration of the organic and aqueous phase was seen, as depicted in Fig. 7(b), indicating that metal ions and TCPP had interacted at the interface of two immiscible solvents. Large and free-standing Cu-MOF membranes that had developed at the contact were transferred to a glass slide, where optical microscopy revealed a claret-colored membrane with a rough surface, as illustrated in Fig. 7(c). Cu-MOF membranes' PXRD spectrum revealed four characteristic peaks - (100), (110), (002), and (004), which were closely matched to their bulk MOF counterparts and therefore suggested that they had a comparable crystal structure, represented in Fig. 7(d).

A subphase of metal ion joints (aqueous solution of $Cu(NO)_3.3H_2O$) at the air/water interface of a Langmuir trough is coated with a solution of molecular building blocks (metalloporphyrin, 5,10,15,20-tetrakis(4-carboxyphenyl)-porphyrinato-palladium(II) (PdTCPP) in chloroform/ methanol) was experimentally performed by Makiura and Konovalov [49]. As the surface is compressed to a pressure of 40 mN/m by moving the barrier walls of the trough at a constant speed, the two-dimensional (2D) copper-mediated PdTCPP arrays (NAFS-13) are formed. The surface pressure - mean molecular area (p-A) isotherm is then measured, as shown by the red line in Fig. 7(e). The CoTCPP-py-Cu (NAFS-1), H_2TCPP-Cu (NAFS-2) and NAFS-13 PdTCPP-Cu sheets' observed p-A isotherms are in good agreement, demonstrating that the linkage motif responsible for sheet formation is also the same. In particular, the linking of the tetratopic PdTCPP molecules occurs via copper ion joints, and the resulting arrays lie flat on the air/water interface. The mean molecular area, A measured at the same surface pressure, p was much less when the same PdTCPP solution was applied to a pure water subphase in the Langmuir trough for comparison and compressed at the same barrier speed, represented by the black line in Fig. 7(e).

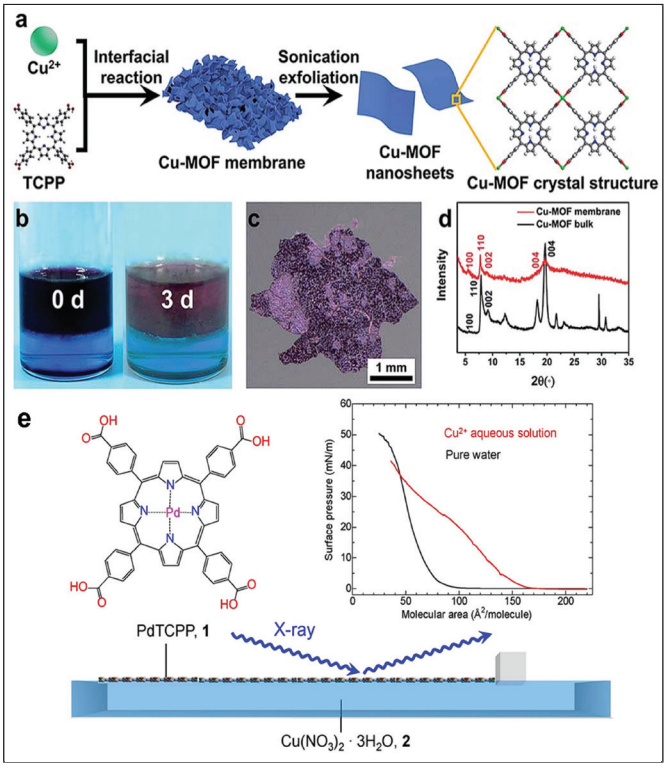


Fig. 7 (a) Synthesis of Cu-MOF nanosheets and crystal structure. [48] (b) Images of two immiscible phases and their color changes both before and after the interaction. (c) A Cu-MOF membrane micrograph. (d) PXRD spectra of bulk analogues of Cu-MOF and a Cu-MOF membrane. (e) PdTCPP-Cu metal-organic framework nanosheets (NAFS-13) assembly is schematically illustrated and is being observed by in-situ grazing incidence XRD (GIXRD) investigations at the air/liquid interface. [49]

2.2.3. Surfactant assisted methods

Surfactant-assisted methods are innovative and versatile approaches for the synthesis of two-dimensional metal-organic frameworks (2D MOFs). These methods utilize surfactants, which are amphiphilic molecules possessing both hydrophilic and hydrophobic segments, to facilitate the controlled formation of 2D MOF nanosheets with specific properties and structures [50–52]. At the heart of these methods is the incorporation of surfactants into the MOF synthesis process. Surfactants play a pivotal role by interacting with both the hydrophilic and hydrophobic components of MOF precursors. They can modify the interfacial properties of the reaction system and impact the nucleation and growth of MOF nanosheets. The surfactant molecules can self-assemble at interfaces, creating a microenvironment that guides the nucleation and growth of MOF nanosheets. Moreover, they can help control the size, shape, and orientation of the resulting nanosheets. Surfactant-assisted methods offer precise control over the growth of 2D MOFs by adjusting surfactant concentration, reaction conditions, and surfactant structure [13,51,53]. These parameters can be fine-tuned to tailor the properties of the synthesized nanosheets, such as size, thickness, porosity, and surface functionality.

Wang et al. used a surfactant-assisted solution synthesis technique to create ultrathin HHB-Cu NSs (hexahydroxybenzene) [2]. The anionic surfactant sodium dodecyl sulfate (SDS) was used for the first time to create consistent, ultrathin 2D c-MOF nanosheets. In a typical synthesis, tetrahydroxy-1,4-quinone (THQ) ligands were added after the $Cu(OAc)_2$ salts and SDS aqueous solution (1.7 mM) were prepared, after which the mixture was sonicated at 50 ºC for 30 minutes. Through electrostatic contact, the SDS molecules' negatively charged hydrophilic tails preferentially cling to the surface of MOFs. As a result, the adsorbed SDS molecules can act as structure-directing agents to significantly reduce layer stacking, which causes the MOFs to develop anisotropically in the 2D direction and, as a result, produce ultrathin and large-sized nanosheets. Additionally, during the sonication treatment, the hydrophobic chains of SDS might reduce the contacts between interlayers, breakdown to create ultrathin nanosheets, and assist stabilize the as-synthesised HHB-Cu MOF NSs in solution to avoid further agglomeration, with the schematic represented in Fig. 8(a).

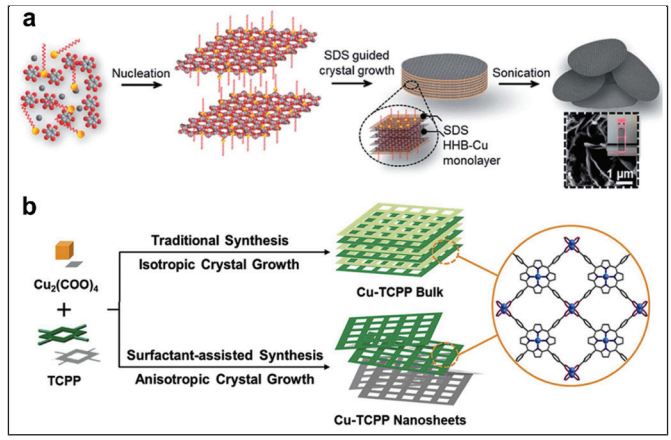


Fig. 8 (a) Using a solution synthesis technique using surfactants, a synthetic approach for ultrathin HHB-Cu NSs is shown. SEM picture of HHB-Cu NSs with the Tyndall effect of a diluent colloidal solution is depicted in the inset. [2] (b) Cu-TCPP MOFs being prepared using conventional and surfactant-aided techniques. [54]

A modified surfactant-assisted technique was used to create Cu-TCPP nanosheets by Qiu et al. [54]. DMF and ethanol were combined at a 3:1 V:V ratio. With magnetic stirring, 300 mL of the aforementioned solution was used to dissolve $Cu(NO_3)_2.3H_2O$, 200 µL of a 1.0 M TFA solution, and 200 mg of PVP, as shown in Fig. 8(b). Additionally, TCPP (100 mg, 0.18 mmol) was dissolved using ultrasound in 100 mL of the produced mixture. TCPP solution was then dropped into the metal-ions solution while being stirred, and the mixture was sonicated for 60 minutes. The completed purple solution was put into a 500 mL sealed container and left at 80 °C for 12 hours. The resultant Cu-TCPP nanosheets were centrifuged at 8000 rpm for 30 minutes before being cleaned with ethanol. Cu-TCPP nanosheets had a 57% yield.

2.2.4. Molecule pre-coordination methods

Bottom-up molecule precoordination methods are innovative approaches in the synthesis of two-dimensional metal-organic frameworks (2D MOFs). These methods enable the controlled assembly of 2D MOF nanosheets by precoordination of metal ions or clusters with organic ligands before the actual framework formation, allowing for precise

control over the structure and properties of the resulting nanosheets [55–57]. To implement this method, suitable metal ions or clusters and organic ligands are carefully chosen based on the desired MOF structure and properties. The precoordination strategy involves designing precursor complexes with a predetermined coordination geometry and ligand binding affinities [58,59].

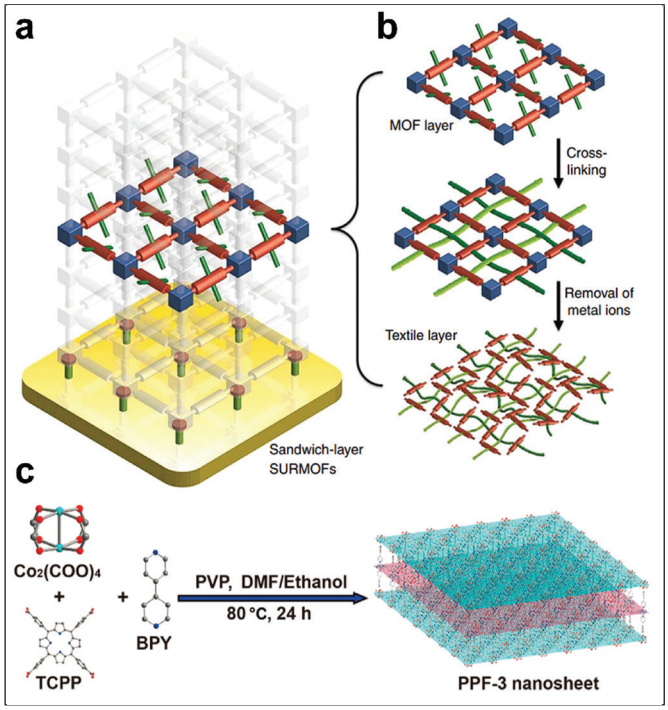


Fig. 9 (a) The heteroepitaxial sandwich-layer surface-mounted MOF (SURMOF) system is shown in a schematic diagram. (b) Cross-linking and metal-removal steps for molecular cross weaving. [60] (c) The development of PPF-3 nanosheets depicted graphically. [61]

A sandwich structure may be created using the molecule pre-coordination method developed by Wang et al. through sandwiching an active layer between two sacrificial layers, shown in Fig. 9(a-b) [60]. By attaching the appropriate node anchoring groups (NAGs), the monomers are properly pre-oriented in the MOF before they polymerize to produce the desired fabric. The crystalline MOF materials are formed by connecting the NAGs to appropriate metal-containing nodes. These 4t-monomers are prearranged in the MOF such that their cross-linking reaction produces flat sheets.

The newly created synthetic approach by Cao et al. was used to successfully create 2D porphyrin paddlewheel framework-3 (PPF-3) MOF nanosheets for the first time [61]. CoSNC, a 2D nanocomposite made of nitrogen-doped carbon and $CoS_{1.097}$ nanoparticles (NPs), is created by simultaneously sulfidating and carbonizing PPF-3 MOF nanosheets. The novel 2D CoSNC nanocomposite was further utilized as an electrode material for supercapacitors as a proof-of-concept application by the group. The formation of 2D PPF-3 nanosheets was controlled by the surfactant molecule polyvinylpyrrolidone (PVP), which was specifically attached to the surface of PPF-3 MOFs in the experiment. In the obtained PPF-3 nanosheet, one 5,10,15,20-tetrakis(4-carboxylphenyl)porphyrin (TCPP) ligand was metalated by one cobalt ion and linked by four $Co_2(COO)_4$ paddlewheel metal nodes to form a "checkerboard-like" layered structure, which was further pillared by 4,4′-bipyridine (BPY) molecules in an AB stacking pattern to form the final structure with space group of *I4/mmm*.

For the production of MOF nanosheets, numerous additional methods, including chemical vapor deposition, hydro- or solvothermal synthesis, etc., have also been reported [62,63]. Post-synthesis pyrolysis of MOFs also represents a transformative approach in tailoring the structure and morphology of carbonaceous materials for advanced applications. This thermal treatment involves subjecting MOF precursors to high temperatures under an inert atmosphere, resulting in the carbonization of organic ligands and the creation of unique carbon-based structures. One of the remarkable outcomes of this process is the retention of the 2D nature of the original MOF, leading to the formation of carbon nanosheets or nanoribbons [64–66]. The preservation of the layered structure is particularly advantageous for applications requiring anisotropic properties and enhanced surface interactions. The pyrolysis-induced carbonization process significantly influences the structural characteristics of the resulting materials. The removal of organic ligands is accompanied by the preservation of inorganic metal nodes, contributing to the formation of carbon frameworks with inherent metal content. This composition may impart additional functionalities to the carbon material, influencing

its chemical and electronic properties. In addition to structural aspects, post-synthesis pyrolysis profoundly impacts the morphology of the carbon materials derived from 2D MOFs. The removal of organic components can create voids or pores within the carbon matrix, leading to the formation of hierarchical porous structures. These structures exhibit interconnected pores at various length scales, offering enhanced surface area and improved accessibility for guest species [65,66]. The resulting hierarchical porosity is particularly advantageous for applications such as gas adsorption, where the tailored pore size distribution facilitates efficient adsorption and desorption processes.

In conclusion, every synthesis technique has advantages and disadvantages. Synthesizing 2D MOFs with desired properties and appropriate for specific applications requires careful process selection and extensive reaction parameter tuning. The discussed synthetic strategies with their individual advantages and limitations are represented in Table 1.

Table 1 Synthetic strategies of 2D MOFs with their key advantages and limitations.

Synthetic method	Advantages	Limitations	References
Physical exfoliation	• Control over Layer Thickness: Physical exfoliation allows precise control over the thickness of the resulting 2D MOF nanosheets. • High Surface Area: The exfoliation process can lead to an increase in the specific surface area of the 2D MOFs. • Enhanced Reactivity: The exposed edges and defects in the exfoliated nanosheets can result in increased reactivity compared to bulk materials. This enhanced reactivity is advantageous for catalytic and sensing applications. • Improved Dispersion: Exfoliated 2D MOF nanosheets can be easily dispersed in various solvents, facilitating their integration into different matrices or devices. This dispersion property enhances the material's applicability in coatings, composites, and films. • Customizable Functionalities: The physical exfoliation method allows for the incorporation of different functional groups during or after the exfoliation process, enabling the customization of the 2D MOF's chemical and physical properties.	• Loss of Crystallinity: The mechanical forces involved in physical exfoliation may lead to a loss of crystallinity in the resulting nanosheets. • Scalability Challenges: Scaling up the physical exfoliation process to produce large quantities of 2D MOF nanosheets can be challenging. The efficiency of the process may decrease at larger scales, limiting the practical applicability for some industrial applications. • Energy Intensive: The physical exfoliation process can be energy-intensive, especially if high shear forces or ultrasonic energy are used. This may affect the overall sustainability and cost-effectiveness of the production process. • Contamination Risk: The introduction of impurities or contaminants during the mechanical exfoliation process can be a concern. This is particularly important for applications requiring high purity, such as in electronic devices. • Limited Control over Orientation: Achieving a specific orientation of the exfoliated nanosheets can be challenging. This lack of control over orientation may impact the material's performance in certain applications.	[67,68]

Synthetic method	Advantages	Limitations	References
Chemical and electrochemical exfoliation	• Precise Control over Thickness: Electrochemical exfoliation enables precise control over layer thickness by adjusting parameters such as applied potential and electrolyte composition. • Preservation of Crystallinity: Chemical and electrochemical exfoliation may better preserve the crystallinity of the 2D MOF layers compared to mechanical methods. • Scalability Potential: Electrochemical methods can be adapted for scalable production, and continuous processes may be developed for industrial-scale production. • Reduced Energy Consumption: In some cases, electrochemical exfoliation methods may have lower energy consumption compared to certain mechanical methods, contributing to sustainability.	• Electrolyte Compatibility: The choice of electrolyte is crucial, and compatibility issues with certain MOFs may limit the applicability of electrochemical exfoliation for specific materials. • Equipment Complexity: Setups can be complex, and the need for specialized equipment may pose challenges, especially for researchers without access to advanced facilities. • Potential Electrode Interference: The presence of electrodes in the electrochemical process may introduce impurities or unwanted reactions, affecting the quality of the exfoliated 2D MOF. • Rate Limiting Steps: The kinetics of the exfoliation process can be a limiting factor, and achieving high production rates may require optimization of reaction conditions.	[63,69]
Template-assisted methods	• Controlled Pore Size and Shape: Template-assisted methods allow for precise control over the pore size and shape of the resulting 2D MOFs. This control is crucial for tailoring the material for specific applications, such as gas adsorption or catalysis. • High Surface Area: The templating process can lead to the formation of 2D MOFs with high surface areas, which is advantageous for applications requiring a large surface area for interactions with other substances. • Enhanced Structural Regularity: Using templates helps achieve enhanced structural regularity in the synthesized 2D MOFs, leading to uniform layers and improved crystallinity.	• Template Removal Challenges: The removal of templates after MOF synthesis can be challenging and may require harsh conditions, potentially leading to damage or alterations in the final structure of the 2D MOF. • Limited Templating Materials: The availability of suitable templates can be limited, and the choice of template material may affect the scalability and applicability of the method. • Possibility of Template Residue: Even after template removal, traces of the template material may remain within the MOF structure, posing potential contamination issues and affecting the material's properties. • Complex Synthesis Procedure: Template-assisted methods often involve more complex synthesis procedures compared to some other methods, which may hinder their widespread adoption.	[14, 32-34]

Synthetic method	Advantages	Limitations	References
Template-assisted methods	• Ordered Nanostructures: Template-assisted methods can result in the formation of ordered nanostructures, such as nanosheets or nanoribbons, which can exhibit unique properties and behaviors compared to disordered structures. • Multifunctionality: The use of templates allows for the incorporation of multiple components or functionalities, enabling the design of multifunctional 2D MOF materials for diverse applications.	• Less Control Over Layer Thickness: Achieving precise control over the layer thickness in template-assisted methods can be challenging compared to top-down methods, limiting the tunability of certain properties. • Limited Scalability: The scalability of template-assisted methods may be limited, particularly when dealing with intricate templates or when attempting to produce large quantities of 2D MOFs.	[14, 32-34]
Interfacial or intermediate layer growth methods	• Controlled Layer Thickness: Interfacial or intermediate layer growth methods allow for precise control over the thickness of the 2D MOF layers. • Uniform and Ordered Structures: These methods often result in the formation of uniform and ordered structures, with well-defined layer arrangements. This structural regularity can lead to improved crystallinity and enhanced material properties. • Versatility in Substrate Choice: Interfacial growth methods can be applied on a variety of substrates, providing versatility in terms of the materials and surfaces on which the 2D MOF layers can be grown. • Potential for Multilayered Structures: The growth process allows for the creation of multilayered structures with controlled interlayer distances, enabling the design of materials with specific functionalities. • Incorporation of Additional Components: Intermediate layer growth methods provide opportunities to incorporate additional components or functionalities during the growth process, leading to multifunctional 2D MOF materials.	• Limited Scalability: The scalability of layer growth methods may be limited, especially when dealing with complex substrates or intricate growth conditions. • Substrate Compatibility: The choice of substrate is critical, and not all substrates are compatible with these methods. Ensuring good adhesion and uniform growth can be challenging on certain surfaces. • Dependence on Interfacial Chemistry: The success of interfacial growth methods often depends on the specific chemistry at the interface. Variations in interfacial conditions can lead to non-uniform growth or incomplete coverage. • Limited Variety of Intermediate Layers: The range of materials that can be used as intermediate layers may be limited, restricting the variety of 2D MOFs that can be synthesized using this approach. • Possible Intercalation Challenges: Achieving controlled intercalation between layers may be challenging, and undesired interactions between adjacent layers may occur, affecting the material's properties. • Template Removal Issues: Similar to other bottom-up methods, the removal of templates or intermediate layers after MOF synthesis can be challenging and may require harsh conditions.	[14,36,37,40,41]

Synthetic method	Advantages	Limitations	References
Surfactant assisted methods	• Controlled Morphology and Size: Surfactants can act as shape-directing agents, allowing for the controlled morphology and size of the resulting 2D MOF structures. • Improved Dispersion: Surfactants can enhance the dispersion of 2D MOFs in solution, leading to more uniform and stable suspensions. This property is advantageous for subsequent processing and applications such as coatings and films. • Stabilization of Intermediates: Surfactants can stabilize intermediate species during the MOF synthesis, preventing uncontrolled aggregation and promoting the formation of well-defined 2D structures. • Tunable Surface Chemistry: The choice of surfactant can allow for the introduction of specific functional groups or surface modifications on the 2D MOF. • Facilitates Nucleation and Growth: Surfactants can act as templates or nucleation sites, promoting the controlled growth of 2D MOF layers and preventing uncontrolled crystal growth.	• Surfactant Removal Challenges: The removal of surfactants after MOF synthesis can be challenging and may require additional purification steps, potentially impacting the final structure and properties of the 2D MOF. • Potential Contamination: Residual surfactants in the final 2D MOF product may lead to contamination, affecting the material's purity and performance in applications where high purity is essential. • Surfactant-Sensitive Synthesis Conditions: The effectiveness of surfactants may be sensitive to synthesis conditions and optimizing these conditions for specific MOFs can be challenging. • Limited Control Over Layer Thickness: Achieving precise control over the layer thickness may be challenging in some cases, as surfactant-assisted methods may result in variations in layer thickness. • Compatibility Issues with Some MOFs: Not all MOFs may be compatible with surfactant-assisted methods, limiting the range of materials that can be synthesized using this approach.	[62]
Molecule pre-coor-dination methods	• Enhanced Control Over Coordination Environment: Molecule precoordination allows for precise control over the coordination environment of metal ions, influencing the subsequent formation of 2D MOF structures with tailored properties. • Improved Crystallinity: Precoordination can lead to improved crystallinity in the resulting 2D MOF, as the controlled coordination of metal ions with ligands can promote the formation of well-defined and ordered structures.	• Complex Synthesis Process: Molecule precoordination methods often involve complex synthesis procedures, requiring precise control over reaction conditions. This complexity may limit the practicality of these methods for large-scale production. • Limited Metal and Ligand Compatibility: The choice of metal ions and ligands for precoordination may be limited by their compatibility with the desired 2D MOF structure. Finding suitable combinations can be a challenge for certain applications.	[47,49,50-53]

Synthetic method	Advantages	Limitations	References
Molecule pre-coordination methods	• Facilitated Nucleation and Growth: Precoordination may act as a nucleation step, providing a favorable environment for the subsequent growth of 2D MOF layers. • Controlled Morphology and Size: The precoordination step can influence the morphology and size of the final 2D MOF, allowing for better control over these structural aspects for specific applications. • Tunable Properties: By carefully selecting the metal ions and ligands during the precoordination step, it is possible to tune the physical and chemical properties of the resulting 2D MOF, making it suitable for various applications.	• Precursor Stability Issues: The stability of precoordination precursors may be a concern, as certain combinations may be prone to decomposition or side reactions, affecting the overall success of the synthesis. • Template Removal Challenges: Similar to other bottom-up methods, the removal of templates or precursors after MOF synthesis can be challenging and may require careful optimization to avoid damage to the final 2D MOF structure. • Scale-Up Challenges: Scaling up molecule precoordination methods for large-scale production may be challenging due to the intricate control needed over precursor stability, reaction conditions, and other parameters.	[47,49,50-53]

3. 2D MOFs for electrochemical energy storage

3.1 Applications of 2D MOFs in supercapacitors

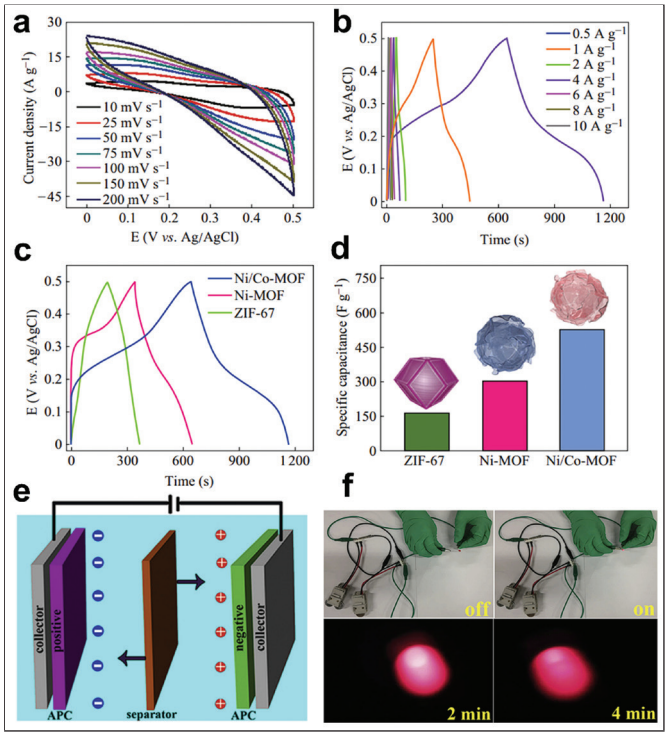


Fig. 10 (a) Cyclic voltammograms of Ni/Co-MOF nanoflake electrodes in 1 M LiOH solution at various scan speeds. (b) Ni/Co-MOF nanoflakes' galvanostatic charge-discharge curves at various currents in 1 M LiOH solution. (c) Ni/Co-MOF nanoflakes, ZIF-67, and Ni/Co-MOF nanoflakes at different current densities in 1 M LiOH solution are compared using galvanostatic charge-discharge curves. (d) Ni/Co-MOF nanoflakes, Ni-MOF nanoflakes, and ZIF-67 electrodes' individual capacitances at 0.5 Ag^{-1}. [70] (e) Schematic of activated porous carbon-based symmetric supercapacitor (SSC) (f) Glowing of LED using the SSC. [71]

Two-dimensional metal-organic frameworks have gained significant attention in the field of supercapacitors due to their unique properties and potential for energy storage applications [3,72]. The distinctive structure of both Ni/Co-MOF nanoflakes and Ni-MOF nanoflakes intrigued Xia et al. to assess their electrochemical performance in the context of a supercapacitor using a three-electrode system in a 1 M LiOH aqueous electrolyte [70]. As depicted in Fig. 10(a), the cyclic voltammetry (CV) curves of the Ni/Co-MOF nanoflakes exhibit approximately rectangular shapes with reversible peaks, indicative of a combination of electric double-layer capacitance (EDLC) and pseudocapacitive reactions [73,74]. Importantly, it is worth noting that even at a high potential scan rate of 200 mVs^{-1}, the roughly rectangular shape of the Ni/Co-MOF nanoflake

CVs is preserved, suggesting a predominantly EDLC behavior and the rapid establishment of the double layer, even under high-rate conditions. The nearly symmetric galvanostatic charge-discharge curves presented in Fig. 10(b) imply that this unique electrode experiences low polarization and exhibits high charge-discharge columbic efficiency. Remarkably, as depicted in Figs. 10(c, d), the Ni/Co-MOF nanoflakes demonstrate a remarkable specific capacitance of 530.4 Fg^{-1} at 0.5 Ag^{-1}, surpassing the specific capacitance values of the Ni-MOF nanoflakes (306.8 Fg^{-1}) and ZIF-67 (168.3 Fg^{-1}) by factors of 3.15 and 1.72, respectively.

In a study by Li et al., a novel Cu-based Metal-Organic Framework (Cu-MOF) with a translational 2D structure characterized by (4,4) layers have been designed [71]. This MOF exhibits hierarchical stacking lamellae with spaces in between, represented in Fig. 10(e). Initially, Cu-MOF was used as a precursor to synthesize a Cu@C composite through a process involving calcination and thermolysis. Subsequently, the Cu@C composite underwent etching with HCl and activation using KOH to yield an Activated Porous Carbon (APC) material with a nanosheet morphology. Notably, this APC nanosheet possessed an exceptionally high BET specific surface area of 2491 m^2/g and a pore volume of 1.50 cm^3/g (comprising 0.12 cm^3/g of micropores and 1.38 cm^3/g of meso- and macropores). Importantly, the APC nanosheet exhibits an impressive specific capacitance of 260.5 F/g when tested at 0.5 A/g with a mass loading of 8 mg/cm^2. The resulting Symmetric Supercapacitor (SSC) based on APC achieves an outstanding specific energy density of 18.38 Wh/kg at a specific power density of 350 W/kg. Moreover, this SSC retains 91.1% of its original capacitance even after undergoing 5000 charge-discharge cycles, demonstrating remarkable long-term cycling stability and reversibility. Remarkably, using three of these SSCs can power a red LED for over 12 minutes, as shown in Fig. 10(f). Consequently, the APC nanosheet emerges as a strong and promising candidate for the fabrication of high-performance supercapacitor cells. The major MOFs used in supercapacitors have been tabulated in terms of porosity, specific surface area, specific capacitance, and retention in Table 2.

Table 2 Material parameters of major MOFs used in supercapacitors.

Material	Pore size (nm)	Specific surface area (m^2/g)	Specific capacitance	Retention (%/ cycles)	Reference
Co-BDC NSs	Broad	260	1159 @ 0.5 A/g, 1052 @ 5 A/g	96.7/6000	[75]
Co-BTC/D-E	Broad	23.1	958.1 @ 2 A/g, 627.6 @ 30 A/g	92.3/3000	[76]
2D Ni-HAB MOFs	0.87 and >15	180-350	420 @ 1 mV/s, 273 @ 100 mV/s	90/12000	[77]
Zn-doped Ni-PTA (MOF-2)	Broad	47.9	1620 @ 0.25 A/g, 854 @ 10 A/g	91/3000	[78]
437-MOF (In)	2.8 and 3.6	2379	150.2 @ 0.2 A/g, 56 @ 8 A/g	~100/6000	[79]
ZnO/NiO MSs (ZnNi-BTC)	7.5-25	170	172.9 @ 0.5 A/g, 107.8 @ 3 A/g	97.4/2000	[80]
NiCo-O (CoNi-MOF-74)	Broad	77.3	305 @ 1 A/g, 218 @ 10 A/g	90.5/10000	[21]
Double shelled Zn-Co-S RDCs (CoZn-ZIF-8)	-	-	1266 @ 1 A/g, 720 @ 20 A/g	91/10000	[81]
Hollow porous NiPO (Ni-BTC)	Broad	142.2	1627 @ 1 A/g, 1044.4 @ 20 A/g	76.8/2000	[19]
Activated porous carbon NSs APC (Cu-BIB)	<6	2491	260.5 @ 0.5 A/g, 165 @ 10 A/g	91.1/5000	[82]
Carbon nanocubes CNC (Zn-BIM)	Broad	1132	255 @ 0.5 A/g, 130 @ 20 A/g	98.2/5000	[83]
2D Ni/Co-MOF nanoflakes	Broad	-	530.4 @ 0.5 A/g	99.75/2000	[84]

3.2. Applications of 2D MOFs in batteries

2D MOFs offer a versatile platform for enhancing various aspects of battery technology, including energy density, rate capability, safety, and cycle life [85–87]. Their versatility, tunability, and unique properties make them a promising avenue for advancing the next generation of energy storage systems.

The exceptional stability and enhanced energy density of lithium-ion batteries have prompted extensive research [88–91]. However, there are numerous issues with the application process, including poor rate performance, low specific capacity, and significant electrode volume expansion. The capacity contribution of lithium/potassium ion batteries can be explained by two primary storage mechanisms for the anode materials: the diffusion-controlled intercalation process and the capacitive process, which is dominated by surface-induced capacitance [92,93]. 2D MOFs with an ultrathin nanosheet structure have emerged as an attempt to increase the number of active sites for the lithium-ion reaction and enhance its specific capacity even further. Because of its high porosity, large specific surface area, enough redox-active metal sites, and short ion diffusion distance, two-dimensional metal-organic frameworks (MOFs) have garnered significant interest as electrode materials for lithium-ion batteries.

2D Cu-BDC MOF nanosheets were meticulously designed and synthesized by precise control of the reaction duration, carried out by Zheng et al. [94]. Subsequently, they underwent annealing at varying pyrolysis temperatures. The end result was the production of MOF-derived carbon materials, namely C500 (referring to the final product obtained at 500°C) and C700 (the final product obtained at 700°C), which were achieved through acid etching. Both carbon derivatives exhibited an abundance of mesoporous structures, which are highly advantageous for facilitating ion migration and promoting the storage of lithium and potassium ions. In the context of lithium-ion and potassium-ion batteries, C500 and C700 displayed distinct dominant kinetic behaviors. Specifically, C500, influenced by a diffusion-controlled process, demonstrated superior performance when employed as an anode material in lithium-ion batteries (LIBs). The C500 anode exhibited an impressive reversible specific capacity of 690.4 milliampere-hours per gram (mAh/g) at a low current density of 0.1 amperes per gram (A/g). Remarkably, even after undergoing 500 charge-discharge cycles at a higher current density of 5.0 A/g, it managed to maintain a substantial specific capacity of 210.3 mAh/g.

Lithium-sulfur (Li-S) batteries hold great potential for the future because of their high theoretical specific capacity (1675 mAh/g) and energy density (2600 Wh/kg) [95,96]. One of the major issues limits the commercialization is the prominent shuttle effect which results from the breakdown of lithium polysulphide and infinite transport/ shuttle between cathode and anode throughout the redox cycle. These occurrences significantly decrease in cycling stability and anode corrosion [96,97]. The breakdown of polysulfide in the organic liquid-based electrolyte is the primary cause of the shuttle effect in Li-S batteries. The physical state of sulfur during the charging and discharging operation will go through a solid-liquid-solid transition process depending on solubility the various sulfur species present in the electrolyte. Elemental sulfur in the solid state will dissolve in the electrolyte and react with the lithium anode to produce low order polysulfide when it is discharged to high order polysulfide. After producing high order polysulfide during charging, the low order polysulfide will then diffuse back to the cathode, and the high order polysulfide will then diffuse to the anode side once more. One practical, yet effective, method to reduce the shuttle effect is to modify the separator. 2D MOF can become a promising candidate as separator or a cathode material which is both chemically and physically and thermally stable, as a physical barrier to prevent soluble polysulfides [97].

While lithium-sulfur (Li-S) batteries offer numerous advantages, such as high energy density, they face practical limitations due to the unwanted shuttle effect and their insulating nature [98]. In response to these

challenges, a conductive metal-organic framework (MOF)-modified separator was developed using a straightforward filtration method by Chen et al. [99]. This modified separator possessed inherent microporous structures, hydrophilic properties, and conductivity, facilitating efficient contact with and retention of polysulfides while promoting faster electrochemical reactions. The physical and chemical attributes of the resulting separator played a crucial role in mitigating the shuttle effect and enhancing the battery's rate capability. Consequently, the Li-S battery equipped with the MOF-modified separator exhibited significantly improved electrochemical performance. Summarily, major 2D MOFs used in batteries have been tabulated and discussed in Table 3, in terms of various parameters.

Table 3 Material parameters of major 2D MOFs used in batteries.

Material	Pore size (nm)	Specific surface area (m^2/g)	Testing potential (V)	Reversible capacity (mAh/g)	Retention (%/cycles)	References
$Cu_3(HHTP)_2$	1.9	506.1	1.7-3.5	95 @ 1 C, 86 @ 20 C	50/500	[100]
Cu-TCA	-	180	1.4-4.3	60 @ 0.5 C, 55 @ 2 C	54.2/200	[91]
Ni-Me4BPZ	Broad	67	0.01-3	140 @ 0.05 A/g	85.7/100	[88]
H-Co-BDC microflowers	5-50	49.9	0.01-3	1345 @ 0.1 A/g, 798 @ 2 A/g	98.8/100	[90]
Mn-BTC	Broad	23.8	0.01-2	694 @ 0.103 A/g, 250 @ 2.06 A/g	83/100	[101]
$AlCl_3$-FumA	Broad	260.1	0.01-3	409 @ 0.0375 A/g, 258 @ 37.5 A/g	93.8/100	[102]
Ti-DOBDC	-	621	0.01-3.0	527 @ 0.1 A/g, 120 @ 0.8 A/g	85/500	[103]
h-ZIF-8@ZnO	1 and 5-8	596.6	0.001-3	805.4 @ 0.2 A/g, 388.6 @ 5 A/g	92.7/100	[104]
ZnO/C NCs (Zn-BDC)	Broad	110	0.01-3	750 @ 0.1 A/g, 351 @ 2 A/g	74.3/100	[105]
CoO@C dandelions (Co-BDC)	~4 and 14	60.3	0.01-3	866 @ 0.1 A/g, 400 @ 5 A/g	110/300	[106]
N-C-800 (ZIF-8)	2	730.1	0.01-3	2037 @ 0.1 A/g, 780 @ 5 A/g	99.2/50	[107]
Zn(BIM)(OAc)	Broad	1535.2	0.001-3	1200 @ 0.1 A/g, 553 @ 10 A/g	110.1/1000	[108]

4. Conclusions and future perspectives

Two-dimensional metal-organic frameworks (2D MOFs) have emerged as promising materials for electrochemical energy storage applications, including batteries and supercapacitors. Their unique properties, such as high surface area, tunable porosity, and versatile chemistry, make them attractive candidates for addressing the growing demand for high-performance and sustainable energy storage solutions. In recent years, significant progress has been made in the synthesis, characterization, and application of 2D MOFs in energy storage systems. These materials have demonstrated impressive performance in terms of energy density, rate capability, and long-term stability. However, several challenges and limitations still need to be addressed to fully unlock their potential.

Future Perspectives:

- Synthesis and Scalability: Developing scalable and cost-effective synthesis methods for large-scale production of 2D MOFs is crucial for practical applications. Exploring innovative techniques and improving the reproducibility of synthesis processes will be a focus area.
- Structural Design: Tailoring the structure of 2D MOFs by fine-tuning metal ions and organic linkers will continue to be explored. Design strategies that enhance ion transport and diffusion within the material while maintaining stability are essential.

- Stability and Durability: Ensuring the long-term stability and durability of 2D MOFs in real-world applications remains a challenge. Research efforts should focus on mitigating degradation mechanisms, particularly in aqueous environments.
- Integration with Current Technologies: Integrating 2D MOFs with existing battery and supercapacitor technologies is crucial for practical implementation. Compatibility with different electrode materials and electrolytes needs further investigation.
- Electrical Conductivity: Improving the electrical conductivity of 2D MOFs is essential for enhancing their rate performance. Strategies such as incorporating conductive additives or creating hybrid materials should be explored.

Challenges and Limitations:

- Low Energy Density: 2D MOFs, like other porous materials, often have lower energy density compared to traditional battery materials. Finding ways to increase their energy density without sacrificing other performance metrics is a challenge.
- Synthesis Control: Achieving precise control over the synthesis of 2D MOFs, including size, shape, and composition, can be challenging. Variability in synthesis can affect their performance.
- Scalability: Transitioning from laboratory-scale synthesis to large-scale production of 2D MOFs can present scalability issues and cost challenges that need to be addressed.
- Structural Stability: Some 2D MOFs may suffer from structural instability during cycling, which can limit their long-term performance. Developing strategies to mitigate this issue is essential.
- Commercial Viability: Demonstrating the commercial viability and cost-effectiveness of 2D MOFs for energy storage applications is a significant hurdle that requires further research and development.

Summarily, 2D MOFs hold great promise for advancing electrochemical energy storage technologies. While substantial progress has been made, addressing the outlined challenges and limitations and pursuing future research directions will be essential to fully harness their potential and facilitate their integration into practical energy storage systems.

Acknowledgements

RM acknowledges CSIR-GATE SRF program for his Ph.D. fellowship. UM is thankful to CSIR, India (Project No. OLP-102) for providing the financial assistance.

Notes

The authors declare no competing financial interests.

References

[1] O.M. Yaghi, G. Li, H. Li, Selective binding and removal of guests in a microporous metal–organic framework, Nature. 378 (1995) 703–706. https://doi.org/10.1038/378703a0.

[2] Z. Wang, G. Wang, H. Qi, M. Wang, M. Wang, S. Park, H. Wang, M. Yu, U. Kaiser, A. Fery, S. Zhou, R. Dong, X. Feng, Ultrathin two-dimensional conjugated metal–organic framework single-crystalline nanosheets enabled by surfactant-assisted synthesis, Chemical Science. 11 (2020) 7665–7671. https://doi.org/10.1039/D0SC01408G.

[3] J. Liu, Y. Zhou, Z. Xie, Y. Li, Y. Liu, J. Sun, Y. Ma, O. Terasaki, L. Chen, Conjugated Copper–Catecholate Framework Electrodes for Efficient Energy Storage, Angewandte Chemie International Edition. 59 (2020) 1081–1086. https://doi.org/10.1002/anie.201912642.

[4] Y. Wang, Z. Deng, J. Huang, H. Li, Z. Li, X. Peng, Y. Tian, J. Lu, H. Tang, L. Chen, Z. Ye, 2D Zr-Fc metal-organic frameworks with highly efficient anchoring and catalytic conversion ability towards polysulfides for advanced Li-S battery, Energy Storage Materials. 36 (2021) 466–477. https://doi.org/10.1016/j.ensm.2021.01.025.

[5] X. Cui, L. Zhang, J. Zhang, L. Gong, M. Gao, P. Zheng, L. Xiang, W. Wang, W. Hu, Q. Xu, W. Wei, H. Zeng, A novel metal-organic layered material with superior supercapacitive performance through ultrafast and reversible tetraethylammonium intercalation, Nano Energy. 59 (2019) 102–109. https://doi.org/10.1016/j.nanoen.2019.02.034.

[6] B. Liu, H. Shioyama, T. Akita, Q. Xu, Metal-Organic Framework as a Template for Porous Carbon Synthesis, Journal of the American Chemical Society. 130 (2008) 5390–5391. https://doi.org/10.1021/ja7106146.

[7] K.J. Erickson, F. Léonard, V. Stavila, M.E. Foster, C.D. Spataru, R.E. Jones, B.M. Foley, P.E. Hopkins, M.D. Allendorf, A.A. Talin, Thin Film Thermoelectric Metal–Organic Framework with High Seebeck Coefficient and Low Thermal Conductivity, Advanced Materials. 27 (2015) 3453–3459. https://doi.org/10.1002/adma.201501078.

[8] X. Song, X. Wang, Y. Li, C. Zheng, B. Zhang, C. Di, F. Li, C. Jin, W. Mi, L. Chen, W. Hu, 2D Semiconducting Metal–Organic Framework Thin Films for Organic Spin Valves, Angewandte Chemie International Edition. 59 (2020) 1118–1123. https://doi.org/10.1002/anie.201911543.

[9] D. Sheberla, J.C. Bachman, J.S. Elias, C.-J. Sun, Y. Shao-Horn, M. Dincă, Conductive MOF electrodes for stable supercapacitors with high areal capacitance, Nature Materials. 16 (2017) 220–224. https://doi.org/10.1038/nmat4766.

[10] T.C. Narayan, T. Miyakai, S. Seki, M. Dincă, High Charge Mobility in a Tetrathiafulvalene-Based Microporous Metal–Organic Framework, Journal of the American Chemical Society. 134 (2012) 12932–12935. https://doi.org/10.1021/ja3059827.

[11] R. Freund, O. Zaremba, G. Arnauts, R. Ameloot, G. Skorupskii, M. Dincă, A. Bavykina, J. Gascon, A. Ejsmont, J. Goscianska, M. Kalmutzki, U. Lächelt, E. Ploetz, C.S. Diercks, S. Wuttke, The Current Status of MOF and COF Applications, Angewandte Chemie International Edition. 60 (2021) 23975–24001. https://doi.org/10.1002/anie.202106259.

[12] J.Wang,N.Li,Y.Xu,H.Pang,Two-Dimensional MOF and COF Nanosheets: Synthesis and Applications in Electrochemistry, Chemistry - A European Journal. 26 (2020) 6402–6422. https://doi.org/10.1002/chem.202000294.

[13] Y. Pan, R. Abazari, J. Yao, J. Gao, Recent progress in 2D metal-organic framework photocatalysts: Synthesis, photocatalytic mechanism and applications, JPhys Energy. 3 (2021). https://doi.org/10.1088/2515-7655/abf721.

[14] K.A.S. Usman, J.W. Maina, S. Seyedin, M.T. Conato, L.M. Payawan, L.F. Dumée, J.M. Razal, Downsizing metal–organic frameworks by bottom-up and top-down methods, NPG Asia Materials. 12 (2020). https://doi.org/10.1038/s41427-020-00240-5.

[15] O. Shekhah, J. Liu, R.A. Fischer, Ch. Wöll, MOF thin films: existing and future applications, Chemical Society Reviews. 40 (2011) 1081. https://doi.org/10.1039/c0cs00147c.

[16] C. Liu, J. Wang, J. Wan, C. Yu, MOF-on-MOF hybrids: Synthesis and applications, Coordination Chemistry Reviews. 432 (2021) 213743. https://doi.org/10.1016/j.ccr.2020.213743.

[17] Q.-Q. Huang, Y.-J. Lin, R. Zheng, W.-H. Deng, C. Kashi, P.N. Kumar, G.-E. Wang, G. Xu, Tunable electrical conductivity of a new 3D MOFs: Cu-TATAB, Inorganic Chemistry Communications. 105 (2019) 119–124. https://doi.org/10.1016/j.inoche.2019.04.037.

[18] Y. Wen, Q. Liu, S. Su, Y. Yang, X. Li, Q.-L. Zhu, X. Wu, Coordination tailoring of water-labile 3D MOFs to fabricate ultrathin 2D MOF nanosheets, Nanoscale. 12 (2020) 12767–12772. https://doi.org/10.1039/D0NR02956D.

[19] R. Bendi, V. Kumar, V. Bhavanasi, K. Parida, P.S. Lee, Metal Organic Framework-Derived Metal Phosphates as Electrode Materials for Supercapacitors, Adv Energy Mater. 6 (2016). https://doi.org/10.1002/aenm.201501833.

[20] D. Sheberla, J.C. Bachman, J.S. Elias, C.-J. Sun, Y. Shao-Horn, M. Dincă, Conductive MOF electrodes for stable supercapacitors with high areal capacitance, Nat Mater. 16 (2017) 220–224. https://doi.org/10.1038/nmat4766.

[21] J. Yu, X. Gao, Z. Cui, Y. Jiao, Q. Zhang, H. Dong, L. Yu, L. Dong, Facile Synthesis of Binary Transition Metal Sulfide Tubes Derived from NiCo-MOF-74 for High-Performance Supercapacitors, Energy Technology. 7 (2019). https://doi.org/10.1002/ente.201900018.

[22] O. Padmaraj, M. Venkateswarlu, N. Satyanarayana, Effect of ZnO filler concentration on the conductivity, structure and morphology of PVdF-HFP nanocomposite solid polymer electrolyte for lithium battery application, Ionics (Kiel). 19 (2013) 1835–1842. https://doi.org/10.1007/s11581-013-0922-1.

[23] Y. Wang, Z. Deng, J. Huang, H. Li, Z. Li, X. Peng, Y. Tian, J. Lu, H. Tang, L. Chen, Z. Ye, 2D Zr-Fc metal-organic frameworks with highly efficient anchoring and catalytic conversion ability towards polysulfides for advanced Li-S battery, Energy Storage Mater. 36 (2021) 466–477. https://doi.org/10.1016/j.ensm.2021.01.025.

[24] K.W. Nam, S.S. Park, R. dos Reis, V.P. Dravid, H. Kim, C.A. Mirkin, J.F. Stoddart, Conductive 2D metal-organic framework for high-performance cathodes in aqueous rechargeable zinc batteries, Nat Commun. 10 (2019) 4948. https://doi.org/10.1038/s41467-019-12857-4.

[25] F. Wang, H. Lu, H. Li, J. Li, L. Wang, D. Han, J. Gao, C. Geng, C. Cui, Z. Zhang, Z. Weng, C. Yang, J. Lu, F. Kang, Q.-H. Yang, Demonstrating U-shaped zinc deposition with 2D metal-organic framework nanoarrays for dendrite-free zinc batteries, Energy Storage Mater. 50 (2022) 641–647. https://doi.org/10.1016/j.ensm.2022.06.005.

[26] M. Yuan, R. Wang, W. Fu, L. Lin, Z. Sun, X. Long, S. Zhang, C. Nan, G. Sun, H. Li, S. Ma, Ultrathin Two-Dimensional Metal–Organic Framework Nanosheets with the Inherent Open Active Sites as Electrocatalysts in Aprotic Li–O 2 Batteries, ACS Appl Mater Interfaces. 11 (2019) 11403–11413. https://doi.org/10.1021/acsami.8b21808.

[27] L. Han, D. Zheng, S. Chen, H. Zheng, J. Ma, A Highly Solvent-Stable Metal–Organic Framework Nanosheet: Morphology Control, Exfoliation, and Luminescent Property, Small. 14 (2018). https://doi.org/10.1002/smll.201703873.

[28] Q. Liu, X. Li, Y. Wen, Q. Xu, X. Wu, Q. Zhu, Twofold Interpenetrated 2D MOF Nanosheets Generated by an Instant In Situ Exfoliation Method: Morphology Control and Fluorescent Sensing, Advanced Materials Interfaces. 7 (2020). https://doi.org/10.1002/admi.202000813.

[29] Y. Peng, Y. Li, Y. Ban, W. Yang, Two-Dimensional Metal–Organic Framework Nanosheets for Membrane-Based Gas Separation, Angewandte Chemie. 129 (2017) 9889–9893. https://doi.org/10.1002/ange.201703959.

[30] L. Han, D. Zheng, S. Chen, H. Zheng, J. Ma, A Highly Solvent-Stable Metal–Organic Framework Nanosheet: Morphology Control, Exfoliation, and Luminescent Property, Small. 14 (2018). https://doi.org/10.1002/smll.201703873.

[31] Y. Peng, Y. Li, Y. Ban, W. Yang, Two-Dimensional Metal–Organic Framework Nanosheets for Membrane-Based Gas Separation, Angewandte Chemie International Edition. 56 (2017) 9757–9761. https://doi.org/10.1002/anie.201703959.

[32] R. Mitra, U. Manju, Negative Capacitance and Intrinsic Ferroelectric Behavior in α-MoO_3 Culminating as a Robust Piezoelectric Energy Harvester, ACS Applied Electronic Materials. 5 (2023) 3130–3143. https://doi.org/10.1021/acsaelm.3c00203.

[33] K.S. Novoselov, A. Mishchenko, A. Carvalho, A.H. Castro Neto, 2D materials and van der Waals heterostructures, Science. 353 (2016). https://doi.org/10.1126/science.aac9439.

[34] M.R. Momeni, Z. Zhang, D. Dell'Angelo, F.A. Shakib, Correction: Gauging van der Waals interactions in aqueous solutions of 2D MOFs: when water likes organic linkers more than open-metal sites, Physical Chemistry Chemical Physics. 24 (2022) 25673–25674. https://doi.org/10.1039/D2CP90191A.

[35] M. Yao, J. Xiu, Q. Huang, W. Li, W. Wu, A. Wu, L. Cao, W. Deng, G. Wang, G. Xu, Van der Waals Heterostructured MOF-on-MOF Thin Films: Cascading Functionality to Realize Advanced Chemiresistive Sensing, Angewandte Chemie. 131 (2019) 15057–15061. https://doi.org/10.1002/ange.201907772.

[36] F. Liu, C. Wang, X. Sui, M.A. Riaz, M. Xu, L. Wei, Y. Chen, Synthesis of graphene materials by electrochemical exfoliation: Recent progress and future potential, Carbon Energy. 1 (2019) 173–199. https://doi.org/10.1002/cey2.14.

[37] Y. Yang, H. Hou, G. Zou, W. Shi, H. Shuai, J. Li, X. Ji, Electrochemical exfoliation of graphene-like two-dimensional nanomaterials, Nanoscale. 11 (2019) 16–33. https://doi.org/10.1039/C8NR08227H.

[38] Y. Ding, Y.-P. Chen, X. Zhang, L. Chen, Z. Dong, H.-L. Jiang, H. Xu, H.-C. Zhou, Controlled Intercalation and Chemical Exfoliation of Layered Metal–Organic Frameworks Using a Chemically Labile Intercalating Agent, Journal of the American Chemical Society. 139 (2017) 9136–9139. https://doi.org/10.1021/jacs.7b04829.

[39] N. Liu, P. Kim, J.H. Kim, J.H. Ye, S. Kim, C.J. Lee, Large-Area Atomically Thin MoS 2 Nanosheets Prepared Using Electrochemical Exfoliation, ACS Nano. 8 (2014) 6902–6910. https://doi.org/10.1021/nn5016242.

[40] Y. Liu, H. Li, Y. Han, X. Lv, H. Hou, Y. Fan, Template-Assisted Synthesis of Co,Mn-MOFs with Magnetic Properties Based on Pyridinedicarboxylic Acid, Crystal Growth & Design. 12 (2012) 3505–3513. https://doi.org/10.1021/cg300237e.

[41] Y. Du, C. Ding, J. Timm, R. Marschall, S. Agarwal, Template-assisted Preparation of Self-standing 2D-MOF Membranes for Application in Cascade Reactions, ChemCatChem. 14 (2022). https://doi.org/10.1002/cctc.202201040.

[42] X. Yan, G. Du, H. Chen, Q. Zhao, Q. Guo, J. Wang, Z. Wang, W. Song, Q. Sheng, Y. Luo, Y. Yuan, T. Yue, Label-free fluorescence aptasensor for the detection of patulin using target-induced DNA gates and TCPP/BDC-NH_2 mixed ligands functionalized Zr-MOF systems, Biosensors and Bioelectronics. 217 (2022) 114723. https://doi.org/10.1016/j.bios.2022.114723.

[43] H.G. Zaman, L. Baloo, S.R. Kutty, M. Altaf, Post Synthetic Modification of NH2-(Zr-MOF) via Rapid Microwave-promoted Synthesis for Effective Adsorption of Pb(II) and Cd(II), Arabian Journal of Chemistry. 16 (2023) 104122. https://doi.org/10.1016/j.arabjc.2022.104122.

[44] H. Wang, Q. Wu, H. Fu, L.-Z. Wu, X. Feng, Controlled growth of organic 2D layered material thin films via interfacial methods, Chemical Communications. 58 (2022) 12384–12398. https://doi.org/10.1039/D2CC03941A.

[45] S. Jiang, X. Shi, Y. Zu, F. Sun, G. Zhu, Interfacial growth of 2D MOF membranes via contra-diffusion for CO_2 separation, Materials Chemistry Frontiers. 5 (2021) 5150–5157. https://doi.org/10.1039/D1QM00154J.

[46] J. Ji, B. Liu, H. Huang, X. Wang, L. Yan, S. Qu, X. Liu, H. Jiang, M. Duan, Y. Li, M. Li, Nondestructive passivation of the TiO 2 electron transport layer in perovskite solar cells by the PEIE-2D MOF interfacial modified layer, Journal of Materials Chemistry C. 9 (2021) 7057–7064. https://doi.org/10.1039/D1TC00036E.

[47] E.A. Flügel, A. Ranft, F. Haase, B. V. Lotsch, Synthetic routes toward MOF nanomorphologies, Journal of Materials Chemistry. 22 (2012) 10119. https://doi.org/10.1039/c2jm15675j.

[48] S. Wu, L. Qin, K. Zhang, Z. Xin, S. Zhao, Ultrathin 2D metal–organic framework nanosheets prepared via sonication exfoliation of membranes from interfacial growth and exhibition of enhanced catalytic activity by their gold nanocomposites, RSC Advances. 9 (2019) 9386–9391. https://doi.org/10.1039/C9RA00662A.

[49] R. Makiura, O. Konovalov, Interfacial growth of large-area single-layer metal-organic framework nanosheets, Scientific Reports. 3 (2013) 2506. https://doi.org/10.1038/srep02506.

[50] C. Avci, Y. Liu, J.A. Pariente, A. Blanco, C. Lopez, I. Imaz, D. Maspoch, Template-Free, Surfactant-Mediated Orientation of Self-Assembled Supercrystals of Metal–Organic Framework Particles, Small. 15 (2019). https://doi.org/10.1002/smll.201902520.

[51] A. Pustovarenko, M.G. Goesten, S. Sachdeva, M. Shan, Z. Amghouz, Y. Belmabkhout, A. Dikhtiarenko, T. Rodenas, D. Keskin, I.K. Voets, B.M. Weckhuysen, M. Eddaoudi, L.C.P.M. de Smet, E.J.R. Sudhölter, F. Kapteijn, B. Seoane, J. Gascon, Nanosheets of Nonlayered Aluminum Metal–Organic Frameworks through a Surfactant-Assisted Method, Advanced Materials. 30 (2018). https://doi.org/10.1002/adma.201707234.

[52] X. Zhang, P. Zhang, C. Chen, J. Zhang, G. Yang, L. Zheng, J. Zhang, B. Han, Fabrication of 2D metal–organic framework nanosheets with tailorable thickness using bio-based surfactants and their application in catalysis, Green Chemistry. 21 (2019) 54–58. https://doi.org/10.1039/C8GC02835D.

[53] R. Marsalek, Particle Size and Zeta Potential of ZnO, APCBEE Procedia. 9 (2014) 13–17. https://doi.org/10.1016/j.apcbee.2014.01.003.

[54] S. Qiu, Y. Su, H. Zhao, L. Wang, Q. Xue, Ultrathin metal-organic framework nanosheets prepared via surfactant-assisted method and exhibition of enhanced anticorrosion for composite coatings, Corrosion Science. 178 (2021) 109090. https://doi.org/10.1016/j.corsci.2020.109090.

[55] D. Zacher, R. Nayuk, R. Schweins, R.A. Fischer, K. Huber, Monitoring the Coordination Modulator Shell at MOF Nanocrystals, Crystal Growth & Design. 14 (2014) 4859–4863. https://doi.org/10.1021/cg501025g.

[56] B. Li, X. You, H. Wu, R. Li, K. Xiao, Y. Ren, H. Wang, S. Song, Y. Wang, Y. Pu, X. Huang, Z. Jiang, A facile metal ion pre-anchored strategy for fabrication of defect-free MOF membranes on polymeric substrates, Journal of Membrane Science. 650 (2022) 120419. https://doi.org/10.1016/j.memsci.2022.120419.

[57] S. Chand, S.C. Pal, D.-W. Lim, K. Otsubo, A. Pal, H. Kitagawa, M.C. Das, A 2D Mg(II)-MOF with High Density of Coordinated Waters as Sole Intrinsic Proton Sources for Ultrahigh Superprotonic Conduction, ACS Materials Letters. 2 (2020) 1343–1350. https://doi.org/10.1021/acsmaterialslett.0c00358.

[58] T. Wu, Y. Shi, Z. Wang, C. Liu, J. Bi, Y. Yu, L. Wu, Unsaturated Ni II Centers Mediated the Coordination Activation of Benzylamine for Enhancing Photocatalytic Activity over Ultrathin Ni MOF-74 Nanosheets, ACS Applied Materials & Interfaces. 13 (2021) 61286–61295. https://doi.org/10.1021/acsami.1c20128.

[59] X. Wang, M. Sun, L. Liu, On the construction and performance of pre-oxidized probe inserted into charged MOF for the in vitro

vitamin C detection: A highly selective emission turn-on sensing, Spectrochimica Acta Part A: Molecular and Biomolecular Spectroscopy. 297 (2023) 122705. https://doi.org/10.1016/j.saa.2023.122705.

[60] Z. Wang, A. Błaszczyk, O. Fuhr, S. Heissler, C. Wöll, M. Mayor, Molecular weaving via surface-templated epitaxy of crystalline coordination networks., Nature Communications. 8 (2017) 14442. https://doi.org/10.1038/ncomms14442.

[61] F. Cao, M. Zhao, Y. Yu, B. Chen, Y. Huang, J. Yang, X. Cao, Q. Lu, X. Zhang, Z. Zhang, C. Tan, H. Zhang, Synthesis of Two-Dimensional CoS 1.097 /Nitrogen-Doped Carbon Nanocomposites Using Metal–Organic Framework Nanosheets as Precursors for Supercapacitor Application, Journal of the American Chemical Society. 138 (2016) 6924–6927. https://doi.org/10.1021/jacs.6b02540.

[62] J. Hwang, A. Ejsmont, R. Freund, J. Goscianska, B.V.K.J. Schmidt, S. Wuttke, Controlling the morphology of metal–organic frameworks and porous carbon materials: metal oxides as primary architecture-directing agents, Chem Soc Rev. 49 (2020) 3348–3422. https://doi.org/10.1039/C9CS00871C.

[63] V.M.V., G. Nageswaran, Review—2D Layered Metal Organic Framework Nanosheets as an Emerging Platform for Electrochemical Sensing, J Electrochem Soc. 167 (2020) 136502. https://doi.org/10.1149/1945-7111/abb4f5.

[64] L. Chai, L. Zhang, X. Wang, L. Xu, C. Han, T.-T. Li, Y. Hu, J. Qian, S. Huang, Bottom-up synthesis of MOF-derived hollow N-doped carbon materials for enhanced ORR performance, Carbon NY. 146 (2019) 248–256. https://doi.org/10.1016/j.carbon.2019.02.006.

[65] K. Zhao, S. Liu, G. Ye, Q. Gan, Z. Zhou, Z. He, High-yield bottom-up synthesis of 2D metal–organic frameworks and their derived ultrathin carbon nanosheets for energy storage, J Mater Chem A Mater. 6 (2018) 2166–2175. https://doi.org/10.1039/C7TA06916B.

[66] Y.-C. Han, M.-L. Liu, L. Sun, X.-C. Li, Y. Yao, C. Zhang, S.-Y. Ding, H.-G. Liao, L. Zhang, F.R. Fan, M. Moskovits, Z.-Q. Tian, A general strategy for overcoming the trade-off between ultrasmall size and high loading of MOF-derived metal nanoparticles by millisecond pyrolysis, Nano Energy. 97 (2022) 107125. https://doi.org/10.1016/j.nanoen.2022.107125.

[67] K. Cheng, Y. Li, Z. Gao, F. Chen, C. You, B. Sun, Two-dimensional metal organic framework for effective gas absorption, Inorg Chem Commun. 101 (2019) 27–31. https://doi.org/10.1016/j.inoche.2018.12.003.

[68] C. Li, C. Wu, B. Zhang, Enhanced CO_2 / CH_4 Separation Performances of Mixed Matrix Membranes Incorporated with Two-Dimensional Ni-Based MOF Nanosheets, ACS Sustain Chem Eng. 8 (2020) 642–648. https://doi.org/10.1021/acssuschemeng.9b06370.

[69] W. Pang, B. Shao, X.-Q. Tan, C. Tang, Z. Zhang, J. Huang, Exfoliation of metal–organic frameworks into efficient single-layer metal–organic nanosheet electrocatalysts by the synergistic action of host–guest interactions and sonication, Nanoscale. 12 (2020) 3623–3629. https://doi.org/10.1039/C9NR09742B.

[70] H. Xia, J. Zhang, Z. Yang, S. Guo, S. Guo, Q. Xu, 2D MOF Nanoflake-Assembled Spherical Microstructures for Enhanced Supercapacitor and Electrocatalysis Performances, Nano-Micro Letters. 9 (2017) 43. https://doi.org/10.1007/s40820-017-0144-6.

[71] Z.-X. Li, B.-L. Yang, K.-Y. Zou, L. Kong, M.-L. Yue, H.-H. Duan, Novel porous carbon nanosheet derived from a 2D Cu-MOF: Ultrahigh porosity and excellent performances in the supercapacitor cell, Carbon. 144 (2019) 540–548. https://doi.org/10.1016/j.carbon.2018.12.061.

[72] W.Y. Chen, S.N. Lai, C.C. Yen, X. Jiang, D. Peroulis, L.A. Stanciu, Surface Functionalization of Ti3C2TxMXene with Highly Reliable Superhydrophobic Protection

for Volatile Organic Compounds Sensing, ACS Nano. 14 (2020) 11490–11501. https://doi.org/10.1021/acsnano.0c03896.

[73] M.A. Borysiewicz, J.-H. Dou, I. Stassen, M. Dincă, Why conductivity is not always king – physical properties governing the capacitance of 2D metal–organic framework-based EDLC supercapacitor electrodes: a Ni 3 (HITP) 2 case study, Faraday Discussions. 231 (2021) 298–304. https://doi.org/10.1039/D1FD00028D.

[74] S. Bi, H. Banda, M. Chen, L. Niu, M. Chen, T. Wu, J. Wang, R. Wang, J. Feng, T. Chen, M. Dincă, A.A. Kornyshev, G. Feng, Molecular understanding of charge storage and charging dynamics in supercapacitors with MOF electrodes and ionic liquid electrolytes, Nature Materials. 19 (2020) 552–558. https://doi.org/10.1038/s41563-019-0598-7.

[75] Y. Zheng, S. Zheng, Y. Xu, H. Xue, C. Liu, H. Pang, Ultrathin two-dimensional cobalt-organic frameworks nanosheets for electrochemical energy storage, Chemical Engineering Journal. 373 (2019) 1319–1328. https://doi.org/10.1016/j.cej.2019.05.145.

[76] R. Ramachandran, C. Zhao, D. Luo, K. Wang, F. Wang, Morphology-dependent electrochemical properties of cobalt-based metal organic frameworks for supercapacitor electrode materials, Electrochim Acta. 267 (2018) 170–180. https://doi.org/10.1016/j.electacta.2018.02.074.

[77] D. Feng, T. Lei, M.R. Lukatskaya, J. Park, Z. Huang, M. Lee, L. Shaw, S. Chen, A.A. Yakovenko, A. Kulkarni, J. Xiao, K. Fredrickson, J.B. Tok, X. Zou, Y. Cui, Z. Bao, Robust and conductive two-dimensional metal−organic frameworks with exceptionally high volumetric and areal capacitance, Nat Energy. 3 (2018) 30–36. https://doi.org/10.1038/s41560-017-0044-5.

[78] J. Yang, C. Zheng, P. Xiong, Y. Li, M. Wei, Zn-doped Ni-MOF material with a high supercapacitive performance, J. Mater. Chem. A. 2 (2014) 19005–19010. https://doi.org/10.1039/C4TA04346D.

[79] M. Du, M. Chen, X.-G. Yang, J. Wen, X. Wang, S.-M. Fang, C.-S. Liu, A channel-type mesoporous In(<scp>iii</scp>)–carboxylate coordination framework with high physicochemical stability for use as an electrode material in supercapacitors, J. Mater. Chem. A. 2 (2014) 9828–9834. https://doi.org/10.1039/C4TA00963K.

[80] L. Zhang, J. Zhang, Y. Liu, L. Zhang, A. Yuan, Porous ZnO/NiO Microspherical Structures Prepared by Thermolysis of Heterobimetallic Metal-Organic Framework as Supercapacitor Electrodes, J Nanosci Nanotechnol. 17 (2017) 2571–2577. https://doi.org/10.1166/jnn.2017.12677.

[81] B. Zhang, Z. Xu, Q. Teng, G. Pan, M. Ma, B. Shen, A Long-Range Acting Dehydratase Domain as the Missing Link for C17-Dehydration in Iso-Migrastatin Biosynthesis, Angewandte Chemie. 129 (2017) 7353–7357. https://doi.org/10.1002/ange.201703588.

[82] Z.-X. Li, B.-L. Yang, K.-Y. Zou, L. Kong, M.-L. Yue, H.-H. Duan, Novel porous carbon nanosheet derived from a 2D Cu-MOF: Ultrahigh porosity and excellent performances in the supercapacitor cell, Carbon N Y. 144 (2019) 540–548. https://doi.org/10.1016/j.carbon.2018.12.061.

[83] K. Zhao, S. Liu, G. Ye, Q. Gan, Z. Zhou, Z. He, High-yield bottom-up synthesis of 2D metal–organic frameworks and their derived ultrathin carbon nanosheets for energy storage, J Mater Chem A Mater. 6 (2018) 2166–2175. https://doi.org/10.1039/C7TA06916B.

[84] H. Xia, J. Zhang, Z. Yang, S. Guo, S. Guo, Q. Xu, 2D MOF Nanoflake-Assembled Spherical Microstructures for Enhanced Supercapacitor and Electrocatalysis Performances, Nanomicro Lett. 9 (2017) 43. https://doi.org/10.1007/s40820-017-0144-6.

[85] K.W. Nam, S.S. Park, R. dos Reis, V.P. Dravid, H. Kim, C.A. Mirkin, J.F. Stoddart, Conductive 2D metal-organic framework for high-performance cathodes in aqueous

rechargeable zinc batteries, Nature Communications. 10 (2019) 4948. https://doi.org/10.1038/s41467-019-12857-4.

[86] X. Wang, C. Zhao, B. Liu, S. Zhao, Y. Zhang, L. Qian, Z. Chen, J. Wang, X. Wang, Z. Chen, Creating Edge Sites within the 2D Metal-Organic Framework Boosts Redox Kinetics in Lithium–Sulfur Batteries, Advanced Energy Materials. 12 (2022). https://doi.org/10.1002/aenm.202201960.

[87] F. Wang, H. Lu, H. Li, J. Li, L. Wang, D. Han, J. Gao, C. Geng, C. Cui, Z. Zhang, Z. Weng, C. Yang, J. Lu, F. Kang, Q.-H. Yang, Demonstrating U-shaped zinc deposition with 2D metal-organic framework nanoarrays for dendrite-free zinc batteries, Energy Storage Materials. 50 (2022) 641–647. https://doi.org/10.1016/j.ensm.2022.06.005.

[88] T. An, Y. Wang, J. Tang, Y. Wang, L. Zhang, G. Zheng, A flexible ligand-based wavy layered metal–organic framework for lithium-ion storage, J Colloid Interface Sci. 445 (2015) 320–325. https://doi.org/10.1016/j.jcis.2015.01.012.

[89] Y. Tong, M. Que, S. Su, L. Chen, Design of amphiphilic poly(vinylidene fluoride-co-hexafluoropropylene)-based gel electrolytes for high-performance lithium-ion batteries, Ionics (Kiel). 22 (2016) 1311–1318. https://doi.org/10.1007/s11581-016-1662-9.

[90] L. Chen, W. Yang, J. Wang, C. Chen, M. Wei, Hierarchical Cobalt-Based Metal–Organic Framework for High-Performance Lithium-Ion Batteries, Chemistry – A European Journal. 24 (2018) 13362–13367. https://doi.org/10.1002/chem.201802629.

[91] Z. Peng, X. Yi, Z. Liu, J. Shang, D. Wang, Triphenylamine-Based Metal–Organic Frameworks as Cathode Materials in Lithium-Ion Batteries with Coexistence of Redox Active Sites, High Working Voltage, and High Rate Stability, ACS Appl Mater Interfaces. 8 (2016) 14578–14585. https://doi.org/10.1021/acsami.6b03418.

[92] X. Wang, C. Zhao, B. Liu, S. Zhao, Y. Zhang, L. Qian, Z. Chen, J. Wang, X. Wang, Z. Chen, Creating Edge Sites within the 2D Metal-Organic Framework Boosts Redox Kinetics in Lithium–Sulfur Batteries, Adv Energy Mater. 12 (2022). https://doi.org/10.1002/aenm.202201960.

[93] H. Chen, Y. Xiao, C. Chen, J. Yang, C. Gao, Y. Chen, J. Wu, Y. Shen, W. Zhang, S. Li, F. Huo, B. Zheng, Conductive MOF-Modified Separator for Mitigating the Shuttle Effect of Lithium–Sulfur Battery through a Filtration Method, ACS Appl Mater Interfaces. 11 (2019) 11459–11465. https://doi.org/10.1021/acsami.8b22564.

[94] G. Zheng, Z. Xing, X. Gao, C. Nie, Z. Xu, Z. Ju, Fabrication of 2D Cu-BDC MOF and its derived porous carbon as anode material for high-performance Li/K-ion batteries, Applied Surface Science. 559 (2021) 149701. https://doi.org/10.1016/j.apsusc.2021.149701.

[95] M. Zhao, B.-Q. Li, X.-Q. Zhang, J.-Q. Huang, Q. Zhang, A Perspective toward Practical Lithium–Sulfur Batteries, ACS Cent Sci. 6 (2020) 1095–1104. https://doi.org/10.1021/acscentsci.0c00449.

[96] A. Manthiram, Y. Fu, Y.-S. Su, Challenges and Prospects of Lithium–Sulfur Batteries, Acc Chem Res. 46 (2013) 1125–1134. https://doi.org/10.1021/ar300179v.

[97] D. Chen, S. Mukherjee, C. Zhang, Y. Li, B. Xiao, C.V. Singh, Two-dimensional square metal organic framework as promising cathode material for lithium-sulfur battery with high theoretical energy density, J Colloid Interface Sci. 613 (2022) 435–446. https://doi.org/10.1016/j.jcis.2021.12.045.

[98] A. Manthiram, Y. Fu, Y.-S. Su, Challenges and Prospects of Lithium–Sulfur Batteries, Accounts of Chemical Research. 46 (2013) 1125–1134. https://doi.org/10.1021/ar300179v.

[99] H. Chen, Y. Xiao, C. Chen, J. Yang, C. Gao, Y. Chen, J. Wu, Y. Shen, W. Zhang, S.

Li, F. Huo, B. Zheng, Conductive MOF-Modified Separator for Mitigating the Shuttle Effect of Lithium–Sulfur Battery through a Filtration Method, ACS Applied Materials & Interfaces. 11 (2019) 11459–11465. https://doi.org/10.1021/acsami.8b22564.

[100] S. Gu, Z. Bai, S. Majumder, B. Huang, G. Chen, Conductive metal–organic framework with redox metal center as cathode for high rate performance lithium ion battery, J Power Sources. 429 (2019) 22–29. https://doi.org/10.1016/j.jpowsour.2019.04.087.

[101] S. Maiti, A. Pramanik, U. Manju, S. Mahanty, Reversible Lithium Storage in Manganese 1,3,5-Benzenetricarboxylate Metal–Organic Framework with High Capacity and Rate Performance, ACS Appl Mater Interfaces. 7 (2015) 16357–16363. https://doi.org/10.1021/acsami.5b03414.

[102] Y. Wang, Q. Qu, G. Liu, V.S. Battaglia, H. Zheng, Aluminum fumarate-based metal organic frameworks with tremella-like structure as ultrafast and stable anode for lithium-ion batteries, Nano Energy. 39 (2017) 200–210. https://doi.org/10.1016/j.nanoen.2017.06.007.

[103] S.-B. Xia, S.-W. Yu, L.-F. Yao, F.-S. Li, X. Li, F.-X. Cheng, X. Shen, C.-K. Sun, H. Guo, J.-J. Liu, Robust hexagonal nut-shaped titanium(IV) MOF with porous structure for ultra-high performance lithium storage, Electrochim Acta. 296 (2019) 746–754. https://doi.org/10.1016/j.electacta.2018.11.135.

[104] Y. Zhang, Y. Lu, S. Feng, D. Liu, Z. Ma, S. Wang, On-site evolution of ultrafine ZnO nanoparticles from hollow metal–organic frameworks for advanced lithium ion battery anodes, J Mater Chem A Mater. 5 (2017) 22512–22518. https://doi.org/10.1039/C7TA08284C.

[105] Y. Song, Y. Chen, J. Wu, Y. Fu, R. Zhou, S. Chen, L. Wang, Hollow metal organic frameworks-derived porous ZnO/C nanocages as anode materials for lithium-ion batteries, J Alloys Compd. 694 (2017) 1246–1253. https://doi.org/10.1016/j.jallcom.2016.10.110.

[106] F. Wu, S. Zhang, B. Xi, Z. Feng, D. Sun, X. Ma, J. Zhang, J. Feng, S. Xiong, Unusual Formation of CoO@C "Dandelions" Derived from 2D Kagóme MOLs for Efficient Lithium Storage, Adv Energy Mater. 8 (2018). https://doi.org/10.1002/aenm.201703242.

[107] F. Zheng, Y. Yang, Q. Chen, High lithium anodic performance of highly nitrogen-doped porous carbon prepared from a metal-organic framework, Nat Commun. 5 (2014) 5261. https://doi.org/10.1038/ncomms6261.

[108] K. Zhao, S. Liu, G. Ye, Q. Gan, Z. Zhou, Z. He, High-yield bottom-up synthesis of 2D metal–organic frameworks and their derived ultrathin carbon nanosheets for energy storage, J Mater Chem A Mater. 6 (2018) 2166–2175. https://doi.org/10.1039/C7TA06916B.